Polymer Journal, Vol. 13, No. 8, pp 755—767 (1981)

Deformation Mechanism of Nylon 6 Spherulites under Uniaxial Stretching†

Masaru MATSUO*

Department of Clothing Science, Faculty of Home Economics, Nara Women's University, Kitauoyanishi-machi, Nara 630, Japan.

Yasuo SEINO, Takeshi WATANABE, Shigeru MORIGUCHI, Fumihiko OZAKI, and Tetsuya OGITA

Department of Textile Engineering, Faculty of Engineering, Yamagata University, 4-3-16, Jonan, Yonezawa 992, Japan.

(Received December 11, 1980)

ABSTRACT: The orientation distribution functions of the (200) and (002) crystal planes of nylon 6 are affected by the degree of crystallinity. As for one specimen with crystallinity 47%, these functions of the (200) and (002) crystal planes have maxima at polar angles $\theta_j=0°$ and $\theta_j=90°$, respectively. By contrast, as for the other specimen with crystallinity 28%, both functions have a maximum at polar angle $\theta_j=90°$. These two orientation modes were analyzed using a deformation mode of nylon 6 spherulites. As for the results, this cause was due to the difference of the orientation mode of crystal *b*-axis, that is, (a) the *b*-axis orientation associated with the rotation of crystallites around its own *c**-axis designating the axis perpendicular to the *a*- and *c*-axes and (b) the *b*-axis orientation associated with random rotation of the crystallites around their own *b*-axis. The type (a) orientation predominates in the case of a crystallinity 47%, while the type (b) orientation does in the case of crystallinity 28%. A light scattering apparatus was made so that the scanning bench (arm) supporting the photomultiplier could be moved horizontally at a desired fixed angle between the bench and the horizontal direction. This apparatus provided detailed information about the morphology and the deformation mechanism of nylon 6 spherulites. The light scattering pattern from nylon 6 spherulites was accounted for by one from the spherulites with a disorder of the optical axis orientation in the angular distribution.

KEY WORDS (200) and (002) Crystal Planes / The *b*-Axis Orientation / Nylon 6 Spherulite / Light Scattering Apparatus / Scanning Bench / Angular Distribution /

Several studies[1-3] on the crystal orientation of semicrystalline polymers under uniaxial stretching have been made in relation to the deformation mechanism of the polymer spherulites. Those studies involved comparisons of observed results with those calculated on a model of spherulitic deformation in terms of the orientation distribution functions of reciprocal lattice vectors of particular crystal plane. This method is suitable for evaluating the orientation mechanism of crystallites when the diffraction intensities from the crystal planes are too weak, except those of one or two crystal planes, to obtain correct and detailed data.

For a better understanding of the crystal orientation within spherulites, it is necessary to obtain an orientation distribution function of the crystallites on the basis of the measurable functions of the reciprocal vectors. This method affords the best means of studying the orientation mechanism of crystallites, because one can directly pursue the

† Presented partly at the 27th Annual Meeting of the Society of Polymer Science, Japan, Tokyo, May 26, 1978 and partly at the 29th Annual Meeting of the Society of Polymer Science, Japan, Kyoto, May 28, 1980.

* To whom all correspondence should be addressed.

crystallite orientation distribution within the spherulites without using a model about the deformation mechanism of the spherulites. This method was proposed by Roe and Krigbaum.[4-6] Recently, Matsuo *et al.* applied this method to study the orientation mechanism of crystallites within polyethylene spherulites[7] as well as to the orientation mode of crystallites of polyethylene crystallized from a stressed polymer melt.[8] Analysis was made using the functions of the reciprocal lattice vectors of 13 crystal planes observed from X-ray diffraction measurement. As for the former, a high-density polyethylene, Sholex 5065, with crystallinity 76% was used as a test specimen. It was found that the deformation mechanism is dependent on the rotation of crystalites around their own *b*-axes associated with lamellar rotation in the equatorial region and also around their own *a*-axes associated with the rotation of the crystallites within the lamellae in the meridian direction. However, crystalline polymers with a lower degree of crystallinity gives incorrect measurement for the functions of reciprocal lattice vectors of few crystal planes by X-ray diffraction technique. This indicates the difficulty in evaluating the crystallite orientation of such polymers in terms of the crystallite orientation distribution function proposed by Roe and Krigbaum.[4-6] Therefore, the orientation behavior of crystallites within nylon 6 spherulites was evaluated by comparing the observed results with the results calculated from a deformation model of spherulites in terms of the orientation functions of the reciprocal lattice vectors of the (200) and (002) crystal planes.

This paper aims to investigate the contribution of hydrogen bonds to the crystalline orientation as well as to the deformation of spherulites using specimens with different degree of crystallinity by means of X-ray diffraction and small angle light scattering techniques, since it has been reported that nylon 6 spherulites form either negatively or positively birefringent spherulites or mixtures depending on crystallization conditions.[9-13] In a study by Keller,[13] for example, using microbeam X-ray diffraction, these phenomena were explained in terms of a specific orientation of the hydrogen bonds, either parallel or perpendicular to the lamellar axis (radial direction of the spherulite), and of additional contributions of the hydrogen bonds to the optical anisotropy of the crystals.

In order to obtain detailed information on the deformation mode of nylon 6 spherulites, the intensity distribution of light scattering pattern was measured by the light-scattering apparatus which was improved in the detection system. This apparatus had two advantages for precise measurements of intensity distribution of somewhat complicated patterns.

TEST SPECIMENS AND EXPERIMENTAL PROCEDURES

Pellets of nylon 6 were melted at 270°C for 30 min in the laboratory press under 200 kg cm^{-2} and quenched in the water at 60°C. The film thickness was 200 μm. In order to obtain high crystallinity, the specimen was held for four hours in nitrogen at 216°C and 1 atm. and moreover was held for an hour in silicon oil at 140°C. The specimen was a little oxidized through the above heat treatment. The annealed specimen was found to have the so-called α-modification of crystal structure from X-ray diffraction measurement, which was termed specimen A. The degree of crystallinity was found to be around 47% from density gradient measurement at 20°C. The specimen obtained was too rigid to stretch at any temperature in a dry atmosphere without necking and oxidation. Hence, the specimens were stretched in hot water at 80°C to extension ratios of $\lambda = 1.25$ and 1.4.

In this measurement, the generator of X-ray was set at 100 milliampere-40 kV and the width of the divergent, scattering, and receiving slits were 1/6°, 1/6°, and 0.15 mm, respectively. The X-ray diffraction measurement was carried out in the horizontal plane of the goniometer with respect to the (200) and (002) crystal planes at a fixed value of θ_j denoting a polar angle between a stretching direction and a reciprocal lattice vector of a given crystal plane. The polar angle θ_j was changed at proper intervals from 0° to 90° This process was achieved by the rotation of the specimen around its thickness direction. The scanning speed with regard to the Bragg angle $2\theta_B$ was one-eight degree per minute. After applying correction to the observed X-ray diffraction intensity (for air scattering, background noise, polarization, and absorption) and substracting the contribution of the amorphous halo from the corrected total intensity curve, the equatorial diffraction curve was obtained as a function of the

Bragg angle $2\theta_B$. This intensity curve is believed to be due to the contribution of the diffraction intensity from the crystalline phase. The intensity curve $I_{crys}(2\theta_B)$ is separated into the contribution from the individual crystal planes on the assumption that each peak has a symmetric form given by a Lorenz function of $2\theta_B$.

The light scattering intensity distribution was measured using this apparatus made at our laboratory. The measuring method using this apparatus is quite different from that already used.[14] Using this apparatus, the scattered intensity can be measured without the rotation of polarizer, sample, and analyzer. This method will be discussed in detail later. Light scattering patterns were obtained with a 50 mW He-Ne gas laser as a light source.

RESULTS AND DISCUSSION

Figure 1 shows experimental and theoretical results for the orientation distribution functions $2\pi q_j(\cos\theta_j)$ of the reciprocal lattice vectors of the (200) and (002) crystal planes at extension ratios of $\lambda=1.25$ and 1.4. As can be seen in Figure 1, the

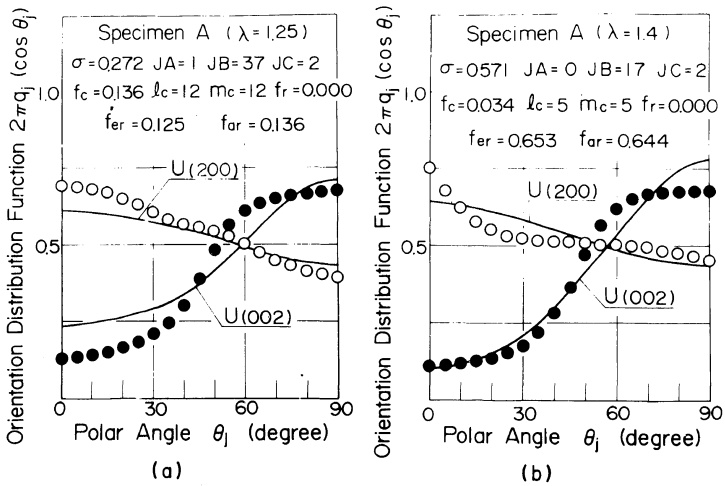

Figure 1. Comparison of orientation distribution functions of the (200) and (002) crystal planes observed with those calculated from eq 1 and 2 for a specimen A: (a) $\lambda=1.25$ and (b) $\lambda=1.4$.

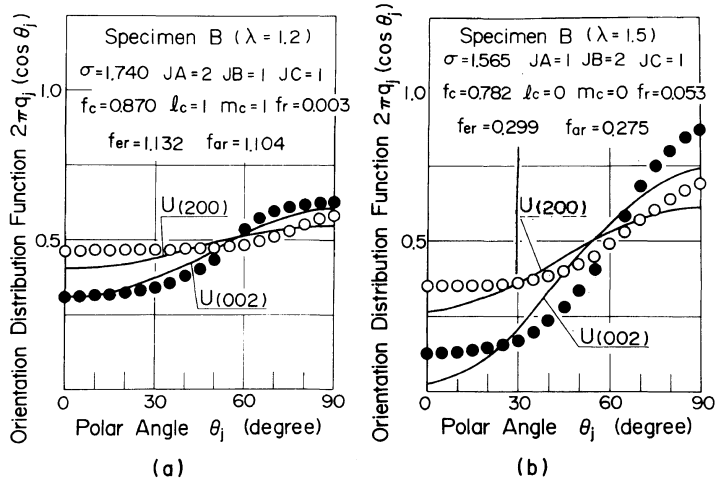

Figure 2. Comparison of the orientation distribution functions of the (200) and (002) crystal planes observed with those calculated from eq 1 and 2 for a specimen B: (a) $\lambda=1.2$ and (b) $\lambda=1.5$.

Table I. Direction of coordinate axes

Coordinate system	Direction of X_i, V_i, and U_i axes	
	$i=1$	$i=3$
$0\text{-}X_1X_2X_3$	Normal to film surface	Stretching direction of film specimen
$0\text{-}V_1V_2V_3$	Normal to lamellar surface containing $0V_2$ and $0V_3$ axes	Lamellar axis grown radially within a spherulite
$0\text{-}U_1U_2U_3$	Crystal *a*-axis of nylon 6 crystallite	Crystal *b*-axis of nylon 6 spherulite

observed distribution function of the (200) crystal plane has the peak at $\theta_j=0°$ and that of the (002) crystal plane at $\theta_j=90°$. This phenomenon seems strange to all appearance, because the molecular axis of nylon 6 crystal unit corresponds to the *b*-axis and therefore the (*h*0*l*) crystal plane is parallel to the molecular axis. Generally speaking, one may presume that the orientation distribution function of the reciprocal lattice vector of the (*h*0*l*) crystal plane has a peak at a higher polar angle θ_j when the molecular axis of crystal unit orient preferentially parallel to the stretching direction. In fact, when the polyethylene spherulites deform under uniaxial stretching to the extension ratio of $\lambda=1.5$, the functions of the (200) and (110) crystal planes have peaks at $\theta_j=90°$ and at around $\theta_j=65°$, respectively.[1-2] Figure 2 shows experimental and theoretical results for the orientation functions of the (200) and (002) crystal planes of nylon 6. These experimental results are the same as those reported by Matsuo *et al.*[3] The specimen B was a melt-extruded and quenched film of nylon 6. The specimen was preheated at about 180°C for 10 min and stretched at 120°C to extension ratios of $\lambda=1.2$ and 1.5. The film specimen thus obtained was annealed at 150°C for 5 min at fixed extension. The annealed specimen was found to have the "so-called" α-modification and the degree of crystallinity was found to be around 28% from density gradient measurement at 20°C. As can be seen in Figure 2, both the experimental distribution functions of the (200) and (002) crystal planes have the peak at $\theta_j=90°$ and this orientation mode is rather close to the crystallite orientation of the fiber texture with symmetrical properties around stretching direction. That is, if both the distribution functions show the same curve, the specimen indicates the ideal fiber texture.

Table II. Euler angles of coordinate transformations

Ref coordinate	Euler angles	Oriented coordinates
$0\text{-}X_1X_2X_3$	θ', ϕ', η	$0\text{-}V_1V_2V_3$
$0\text{-}X_1X_2X_3$	θ, ϕ, η	$0\text{-}U_1U_2U_3$
$0\text{-}V_1V_2V_3$	α, β, γ	$0\text{-}U_1U_2U_3$

Comparing the experimental distribution function in Figure 1 with that in Figure 2, one may postulate the difference of crystallite orientation due to that of degree of crystallinity. Thus, we have tried to demonstrate the difference of crystallite orientation mechanism by comparing the experimental results with the results calculated from a model for a spherulite deformation in terms of the functions of the reciprocal lattice vectors of the (200) and (002) crystal planes.

In accordance with recent studies on the rheo-optical behavior of polymer spherulites,[15-18] two steps in the deformation mechanism may be distinguished: (1) instantaneous deformation of the spherulite, associated with orientation of lamellar axis and untwisting of crystal lamella; (2) reorientation of crystallites within the oriented lamellae after a considerable time lag. The deformation mechanism of nylon 6 spherulites is analyzed by using a model proposed on the basis of the concept of these two steps.

Tables I and II show the geometrical interrelations of three Cartesian system, $0\text{-}X_1X_2X_3$, $0\text{-}V_1V_2V_3$, and $0\text{-}U_1U_2U_3$ fixed within the bulk specimen, crystal lamella, and crystallites, respectively. The directions of the coordinate axes of the each Cartesian system are given in Table I and the Euler angles of coordinate transformations among the three Cartesian systems are given in Table II.

The first step of the spherulite deformation, the instantaneous orientation of crystal lamellae including untwisting, can be represented by the orientation of the Cartesian system 0-$V_1V_2V_3$, with respect to the Cartesian system 0-$X_1X_2X_3$ and can be formulated for uniaxial deformation as follows.[2,7]

$$\omega'(\theta', \eta') = \frac{W_0}{8\pi^2}\{1+\sigma(\lambda-1)(1-\cos^2\theta')\cos^{2J_A}\eta'\} \times \lambda^3/\{\lambda^3-(\lambda^3-1)\cos^2\theta'\}^{3/2} \quad (1)$$

where $\omega'(\theta', \eta')$ is an orientation distribution function of the crystal lamellae with respect to the Cartesian system 0-$X_1X_2X_3$, and σ and J_A are parameters characterizing the ease and sharpness of instantaneous lamellar untwisting, respectively, and W_0 is a normalization constant.

The second step of the spherulite deformation, the delayed reorientation of crystallites within the lamella, can be represented by the orientation of the Cartesian coordinates 0-$U_1U_2U_3$ with respect to the Cartesian coordinates 0-$V_1V_2V_3$. The corresponding distribution function may be formulated as follows.

$$q(\alpha, \beta, \gamma) = \frac{Q_0}{8\pi^2}\{f_r - f_c(\lambda-1)[R(\theta')/R_0]^{J_C}P(\theta') + [(1-\cos^2\beta)\cos^2\alpha\cos^2\gamma]^{J_B} + f_c(\lambda-1)[R(\theta')/R_0]^{J_C}(\sin^4\theta' - \cos^4\beta + 2\cos^2\theta'\cos^2\beta) \times (f_{er}+\cos^{2l_c}\alpha)(f_{ar}+\cos^{2m_c}\gamma)\} \quad (2)$$

In the undeformed state ($\lambda=1$), eq 2 reduces to

$$q(\alpha, \beta, \gamma) = \frac{Q_0}{8\pi^2}\{f_r + [(1-\cos^2\beta)\cos^2\alpha\cos^2\gamma]^{J_B}\} \quad (3)$$

Q_0 is a normalization constant. On the right side of eq 3, the first term ($Q_0f_r/8\pi^2$) corresponds to the fraction of crystallites within the lamella that have random orientation; in the undeformed state, it is the measure of the degree of imperfection of the lamella in the undeformed state. The second term

$$\{Q_0[(1-\cos^2\beta)\cos^2\alpha\cos^2\gamma]^{J_B}/8\pi^2\}$$

corresponds to the fraction of the crystallites with the a-axes oriented parallel to the lamellar axis; this term has a maximum value when the a- and b-axes of the crystal are perfectly oriented in the direction of the lamellar axis (V_3, grown direction) and lamellar normal (V_1, thickness direction), respectively, as listed in Table I. In eq 2 and 3, J_B is a parameter characterizing the sharpness of the distribution function; *i.e.*, J_B is zero or infinite, which means that the orientation is random or perfect, resepctively.

In order to represent the crystal b-axes orientation parallel to the stretching direction due to straining of the tie-chain molecules in the deformed state, the term ($\sin^4\theta' - \cos^4\beta + 2\cos^2\theta'\cos^2\beta$) in eq 2 is introduced in a manner so that the term has a maximum value when the angle β becomes identical to θ' of the lamellar orientation. Two types of the b-axis orientation are postulated on the basis of (a) the b-axis orientation associated with simple rotation of the crystallite around its own c*-axis designating the axis perpendicular to the a- and c-axes and (b) the b-axis orientation associated with the random rotation of the crystallite around its own b-axis. They differ in their effects as indicated by the insertion of the final term in eq 3; *i.e.*, the orientation of type (a) is mostly affected by the factor $\cos^{2l_c}\alpha$ and $\cos^{2m_c}\gamma$, while the orientation of type (b) is affected by the factors f_{er} and f_{ar} in eq 3. In other words, when the factors f_{er} and f_{ar} are zero and the parameters l_c and m_c are infinite, the type (a) orientation is indicated, but, when the values of f_{er} and f_{ar} increase, the type (b) orientation predominates. The parameters l_c and m_c characterize the sharpness of the orientation distribution of the crystallites with respect to the angles α and γ, respectively.

The term $f_c(\lambda-1)[R(\theta')/R_0]^{J_C}$ in eq 2 represents the fractional dependence of the b-axis orientations of both types (a) and (b) on the extension ratio of the spherulite and of the lamella $R(\theta')/R_0$ in terms of the parameters f_c and J_C, where $R(\theta')$ is given by

$$R(\theta') = R_0\lambda\{\lambda^3-(\lambda^3-1)\cos^2\theta'\}^{-1/2} \quad (4)$$

On the other hand, the term $f_c(\lambda-1)[R(\theta')/R_0]^{J_C}P(\theta')$ in eq 2 is added in order to cancel out the variation of the constant Q_0 with the polar angle θ', where $p(\theta')$ is given by

$$P(\theta') = \frac{1}{8\pi^2}\int_0^{2\pi}\int_0^{2\pi}\int_{-1}^{1}(\sin^4\theta' - \cos^4\beta + 2\cos^2\theta'\cos^2\beta)(f_{er}+\cos^{2l_c}\alpha) \times (f_{ar}+\cos^{2m_c}\gamma)\,d(\cos\beta)\,d\alpha\,d\gamma \quad (5)$$

Although the number of parameters in eq 1 and 2

seem to be too large to deduce an explicit conclusion, the values of the parameters giving the best fit of calculated and observed results may also be determined easily using the simplex method.[15]

Actually, the parameters in eq 1 and 2 were determined by an attempt made to minimize the average square error given by the following formula. That is,

$$\text{av sq error} = \frac{\left\{\int_0^{2\pi}\int_0^{\pi} W(\theta_j)\,[q_j(\cos\theta_j)_{\text{exp}} - q_j(\cos\theta_j)_{\text{cal}}]\sin\theta_j\,\mathrm{d}\theta_j\,\mathrm{d}\phi_j\right\}^2}{\left\{\int_0^{2\pi}\int_0^{\pi} q_j(\cos\theta_j)_{\text{exp}}\sin\theta_j\,\mathrm{d}\theta_j\,\mathrm{d}\phi_j\right\}^2} \tag{6}$$

where $W(\theta_j)$ is the weight varied with the polar angle θ_j and is assumed to be unity at any polar angle.

Values of parameters in eq 1 and 2 were shown in Figures 1 and 2. These are the best values as long as eq 1 and 2 are employed as the deformation model of nylon 6 spherulites. Among the values of the parameters f_{er}, f_{ar}, l_c and m_c shown in Figure 1, the values of f_{er} and f_{ar} are somewhat smaller than unity and the value of l_c and m_c are larger than zero. This suggests that the mode of the crystal b-axes orientation in specimen A is hardly affected by the

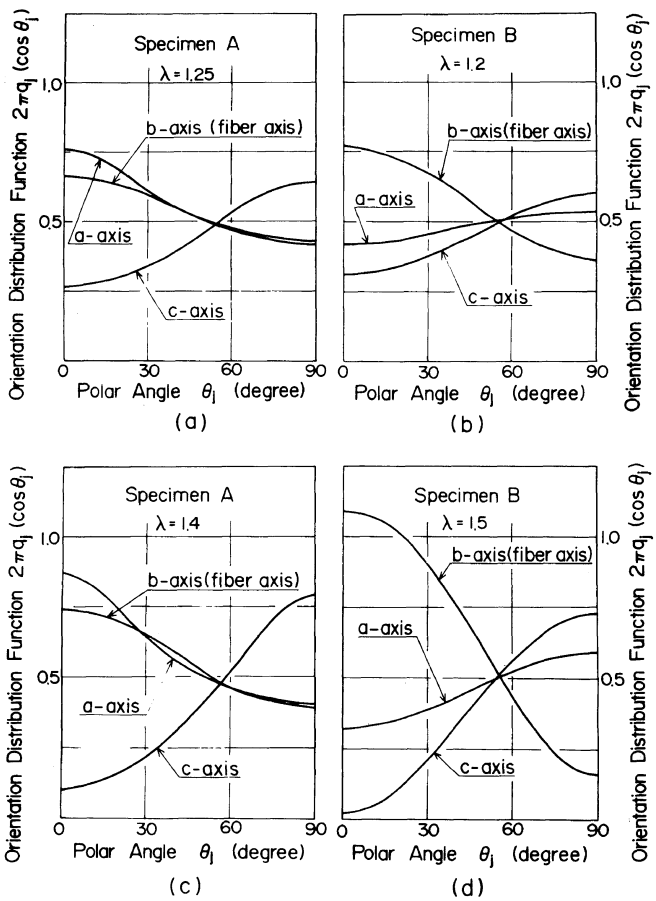

Figure 3. Orientation distribution functions of the crystal a-, b-, and c-axes calculated using the same parameters listed in Figures 1 and 2: (a) Figure 1(a); (b) Figure 1(b); (c) Figure 2(a); (d) Figure 2(b).

random rotation of the crystallites around their own b-axis, but by the rotation of the crystallites around their own c^*-axis.

On the other hand, the values of the parameters l_c and m_c in Figure 2(a) are unity and f_{er} and f_{ar} are larger than unity. In Figure 2(b), the values of parameters l_c and m_c are zero, which indicates random rotation of the crystallites around its own b-axis. This suggests that the crystallite orientation of specimen B is quite different from that of specimen A and the orientation mode of the crystal b-axis under uniaxial stretching is predominanted by the random rotation of the crystallites around their own b-axes. In other words, the crystal orientation of specimen B is somewhat similar to that of the fiber texture whose crystal orientation is random around the crystal fiber axis in a microscopic sense as well as around the stretching direction in a macroscopic one.

Figure 3 shows the orientation functions of the three crystallographic principal axes calculated from the values of the parameters in Figures 1 and 2. The orientation of the crystal b-axes corresponding to the molecular axis indicates the preferential orientation parallel to the stretching direction, while the orientation of the crystal c-axes indicates the preferential orientation perpendicular to the stretching direction, which is independent of the kind of the specimen. On the other hand, the orientation of the crystal a-axes is dependent upon the kind of the specimen. That is, the orientation of specimen A is similar to the crystal b-axes orientation and indicates the preferential orientation to the stretching direction, while that of specimen B is similar to the crystal c-axes orientation. This does not contradict the orientation mode of the crystal (200) and (002) planes shown in Figures 1 and 2. This fact becomes quite clear by obtaining the crystallite orientation function $\omega(\theta, \eta)$.

Figure 4 shows the orientation distribution functions. These orientation functions of specimen B are similar to that of the fiber texture, because the crystallite orientation function about the fiber texture is independent of the angle η and has the

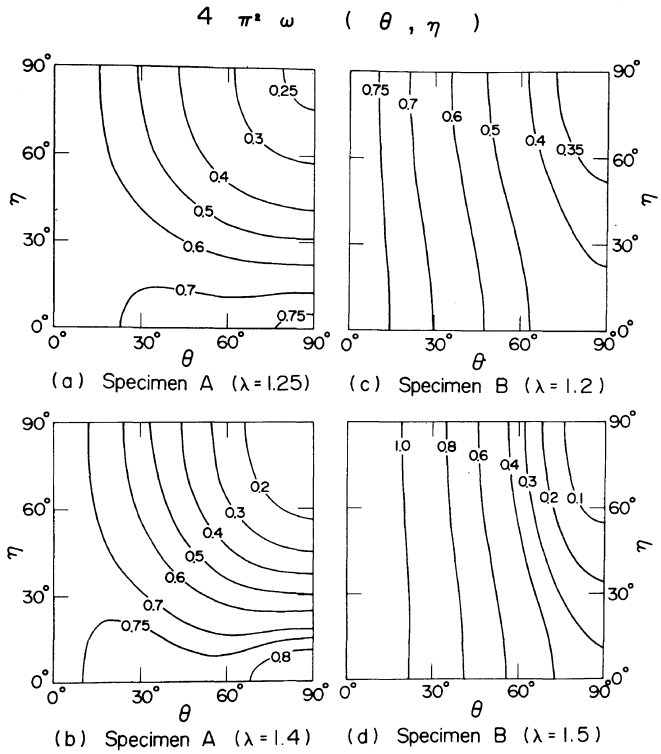

Figure 4. Orientation distribution functions of crystallites calculated using the same parameters listed in Figures 1 and 2: (a) Figure 1(a); (b) Figure 1(b): (c) Figure 2(a); (d) Figure 2(b).

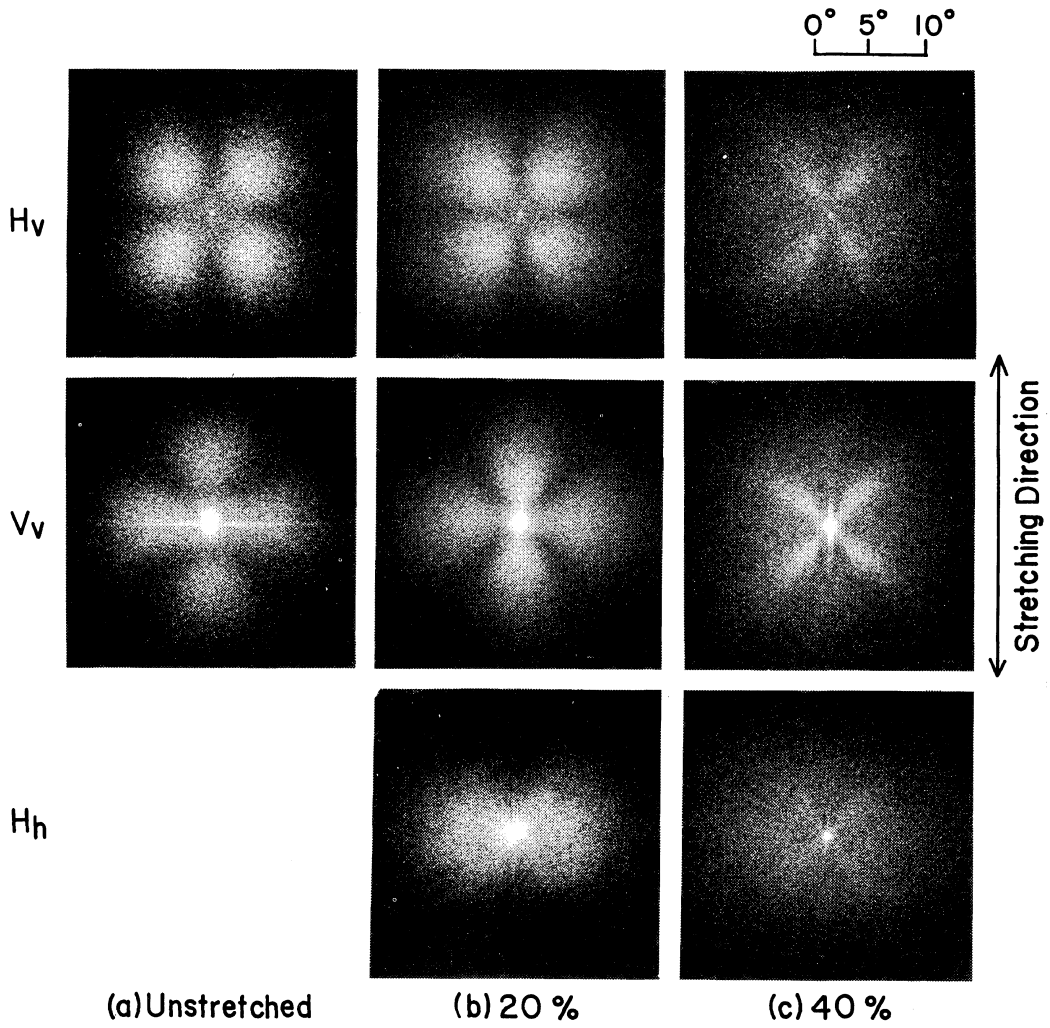

Figure 5. Change in the H_v, V_v, and H_h light scattering patterns with increasing elongation of a specimen A of nylon 6.

maximum at $\theta=0°$. As for the crystallite orientation of specimen A, the density distribution of $\omega(\theta, \eta)$ shows maps with the maxima at $\theta=90°$ and $\eta=0°$. The somewhat complicated maps of specimen A are due to the orientation behavior associated with the crystallite rotation around its own c^*-axis.

Considering the orientation behavior of crystallites within nylon 6 spherulite on the basis of the results shown in Figures 1 through 4, the crystallite orientation seems to be strongly affected by the hydrogen bonds nearly parallel to the crystal a-axes, which is due to crystallinity-dependence of the crystallite orientation. That is, the crystallites within the spherulites having a higher degree of crystallinity such as specimen A seem to be bigger and less disorderly in comparison with those having a lower degree of crystallinity such as specimen B. In the former case, it seems that the stable crystallites are not disintegrated into small fragments by the strain of tie-molecules under uniaxial stretching and consequently the crystal b-axes orient to the stretching direction by the rotation of crystallites around their own c^*-axes. By contrast, in the latter case, the unstable crystallites are postulated to be disintegrated into small fragments by the strain and thus

the preferential orientation of the crystal *b*-axes to the stretching direction may arise with the rotation of crystallites around their own *b*-axes.

Figure 5 shows the photographs of light scattering patterns from spherulites of specimen A under uniaxial stretching. The shapes of the scattering patterns are similar to those of specimen B up to the extension ratio of $\lambda=1.5$ already reported,[3] despite a decided difference in the crystallite orientation mechanism within the deformed spherulites. In a previous paper,[3] the scattering patterns for H_v and V_v polarization were calculated on the basis of the spherulite deformation model by taking the nylon 6 crystals as having orthogonal-biaxial symmetry in optical anisotropy. It was consequently concluded that the H_v scattering can be realized in terms of the proposed model for the spherulitic deformation by taking into account the considerable contribution of hydrogen bonds to the molecular polarizability, so as to make the polarizability along the crystal *a*-axis larger than that along the *b*-axis.

However, the photographic method is insufficient to carry out a detailed analysis of the scattering patterns. Then, we manufactured a trial light scattering apparatus which was improved in the detector system in order to obviate two defects for evaluating the scattered intensity distribution. The measurement for the intensity distribution of the whole scattering pattern has not been correct owing to these two defects. The first is the difficulty in obtaining polarizer, analyzer, and 1/4 wave length plate with satisfactory optical properties. In order to analyze the scattering angle dependence of the scattered intensity, it must be necessary to maintain the equal intensity of an incident beam after passing the polarizer, independent of the rotation of the polarizer. That is, the equal intensity must be maintained despite the change in the polarization condition. Theoretically, this is achieved by the introduction of a 1/4 wave length plate between the laser and polarizer because of the natural polarization property of the laser beam as a source. However, the scattered intensity was found to change with the rotation of the polarizer, which means the experimental impossibility of obtaining the circular polarization condition with the 1/4 wave length plate. This result indicates a serious defect for observing the scattered intensity distribution from polymer films with the provision for rotating the polarization direction by particular angles Ψ_1 and Ψ_2 from the vertical direction. The scattered intensity has been usually measured either in a parallel polarization condition ($\Psi_1=\Psi_2$) in the V_v scattering or in crossed one in the H_v scattering. The second is the difficulty in observing the whole intensity distribution. This defect may not be obviated even if the equal intensity after passing the polarizer is maintained despite rotation of the polarizer. In the previous measurement, we were obliged to use the method shown in Figure 6, in which the lines show the scanning direction of the detector. As can be seen in Figure 6, the scattered intensity was measurable in detail at small scattering angles, but the correct measurement becomes coarse with increasing the scattering angle.

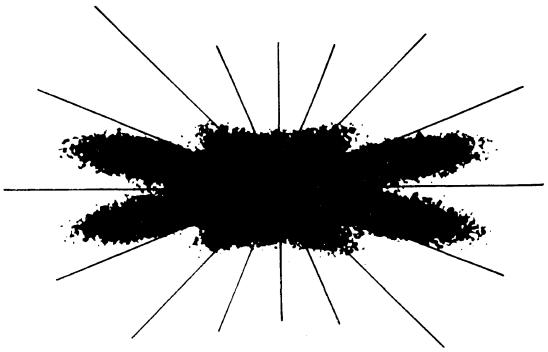

Figure 6. Scanning direction of detector for measuring scattered intensity distribution.

In order to eliminate the above two defects, the light scattering apparatus was manufactured on trial. Figure 7 and 8 show the apparatus and its schematic diagram. The scanning bench (arm) supporting a photomultiplier may be moved horizontally at a desired fixed angle between the bench and the horizontal direction. The fixed angle can be changed at proper intervals from $-5°$ to $35°$. When the experiment was carried out using this apparatus, it is unnecessary to rotate the polarizer, sample, and analyzer at proper intervals about Ψ_1 and Ψ_2 to measure the distribution of the scattered intensity.

Figure 9 shows the scanning direction of the detector using the apparatus. This method is suitable for measuring the scattered intensity distribution of the sharper scattering lobes. Actually, this method obviously provides correct and detailed data in comparison with that in Figure 6.

Figure 10 shows the H_v scattered intensity distribution of a low density polyethylene (Sumikathen

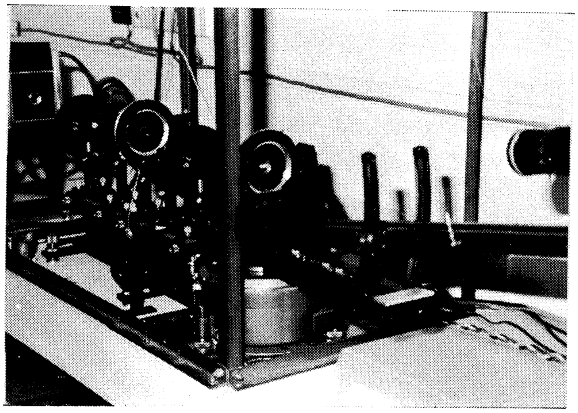

Figure 7. Photograph of light scattering apparatus.

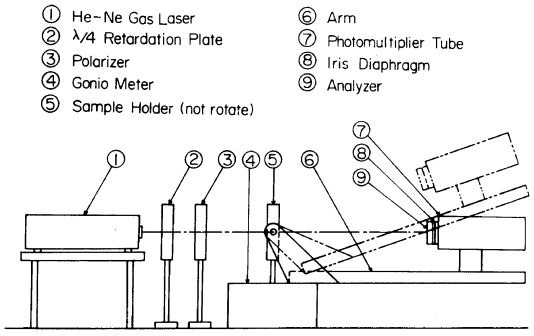

Figure 8. Schematic diagram of light scattering apparatus.

Figure 9. Scanning direction of detector to measure scattered intensity distribution, using the light scattering apparatus shown in Figure 7.

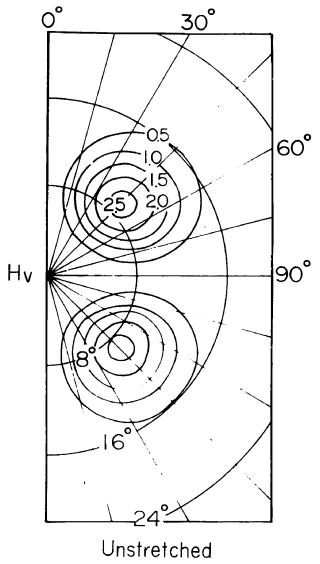

Figure 10. Contour map of scattered intensity distribution of a low density polyethylene (Sumikathen G201) in an undeformed state under H_v polarization conditions.

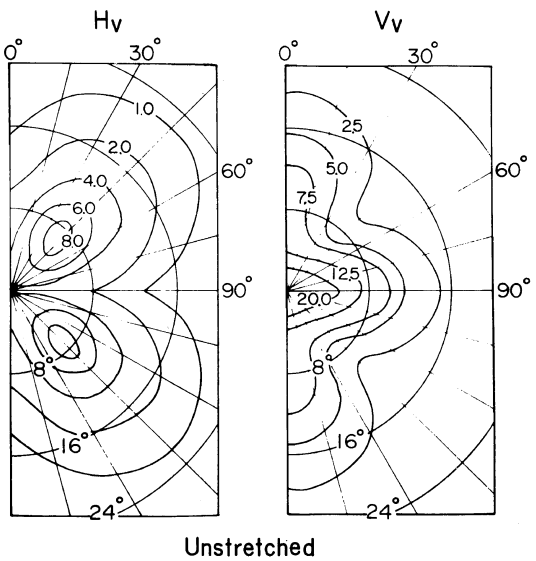

Figure 11. Contour maps of scattered intensity distribution of a specimen A of nylon 6 in an underformed state under H_v and V_v polarization conditions.

G201) in the undeformed state and Figure 11 shows the distributions of nylon 6 under H_v and V_v polarization conditions. These maps were obtained with our apparatus. The H_v scattered intensity in

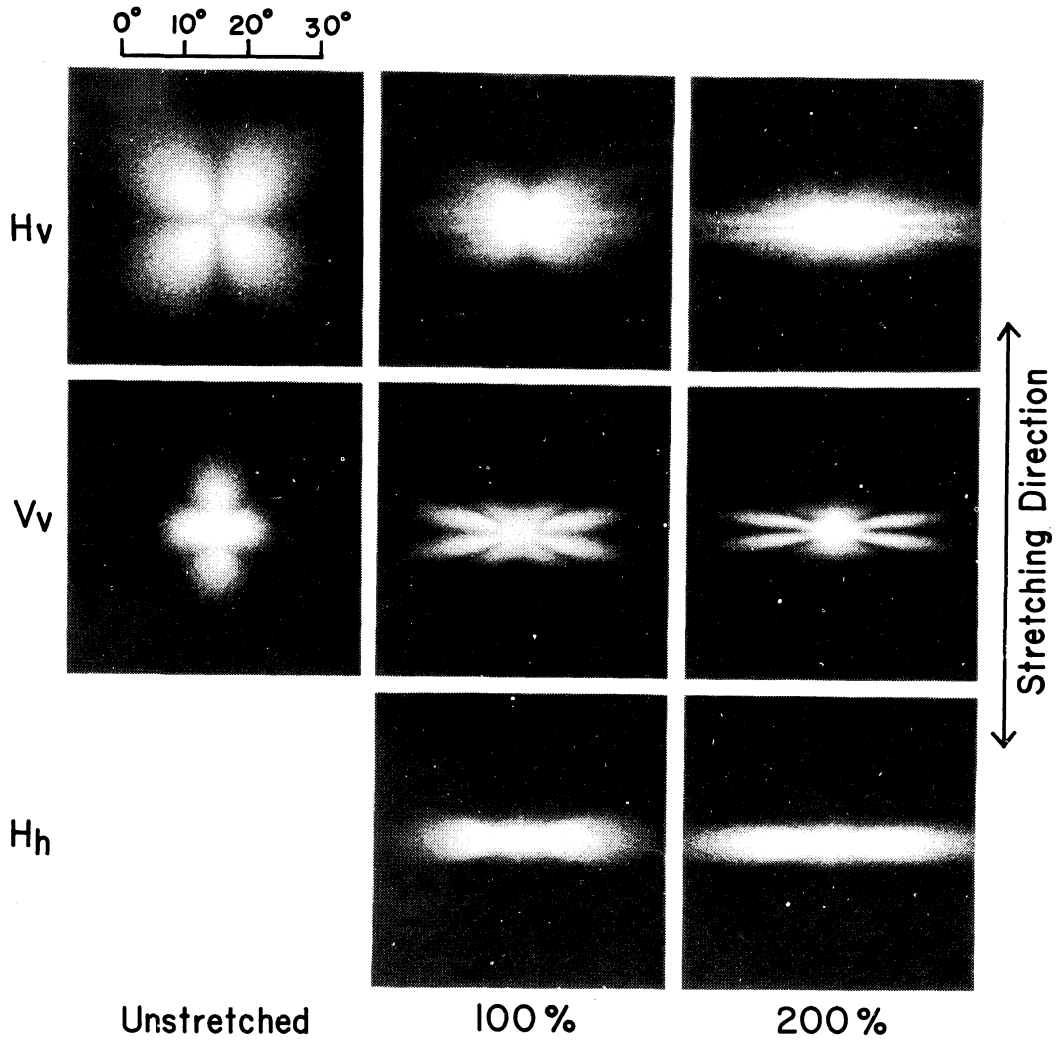

Figure 12. Photographs of light scattering patterns of a specimen B in deformed states of elongation ratios, 100 and 200%, under H_v, V_v, and H_h polarization conditions.

Figure 10 was nearly equal to zero at the scattering angle $\theta=0°$ and at the azimuthal angle $\mu=n\pi/2$ ($n=0\sim3$), while that in Figure 11 was not zero at these angles. This indicates that the polyethylene spherulites are rather close to "perfect spherulites," so termed by Stein and Chu[20] in the case when the orientation of optical axis with respect to the radius is the same everywhere within a spherulite, while the nylon 6 spherulites are rather close to the spherulites having a disorder of the optical axis orientation in the angular direction.[21]

Figures 12 and 13 show the photographs and the contour maps of scattering patterns from nylon 6 spherulites in specimen B at the extension ratios, 100 and 200%, under H_v, V_v, and H_h polarization conditions, respectively. As can be seen the maps in Figure 13, the scattering apparatus provide detailed information on scattered intensity distribution by a comparison of the photographs and the maps. These maps indicate that the deformation mechanism of nylon 6 spherulites cannot be analyzed sufficiently by the deformation model of the perfect spherulites, despite the introduction of the considerable contribution of the hydrogen bonds to the molecular polarizability, so as to make the polarizability along the crystal a-axis larger than that along

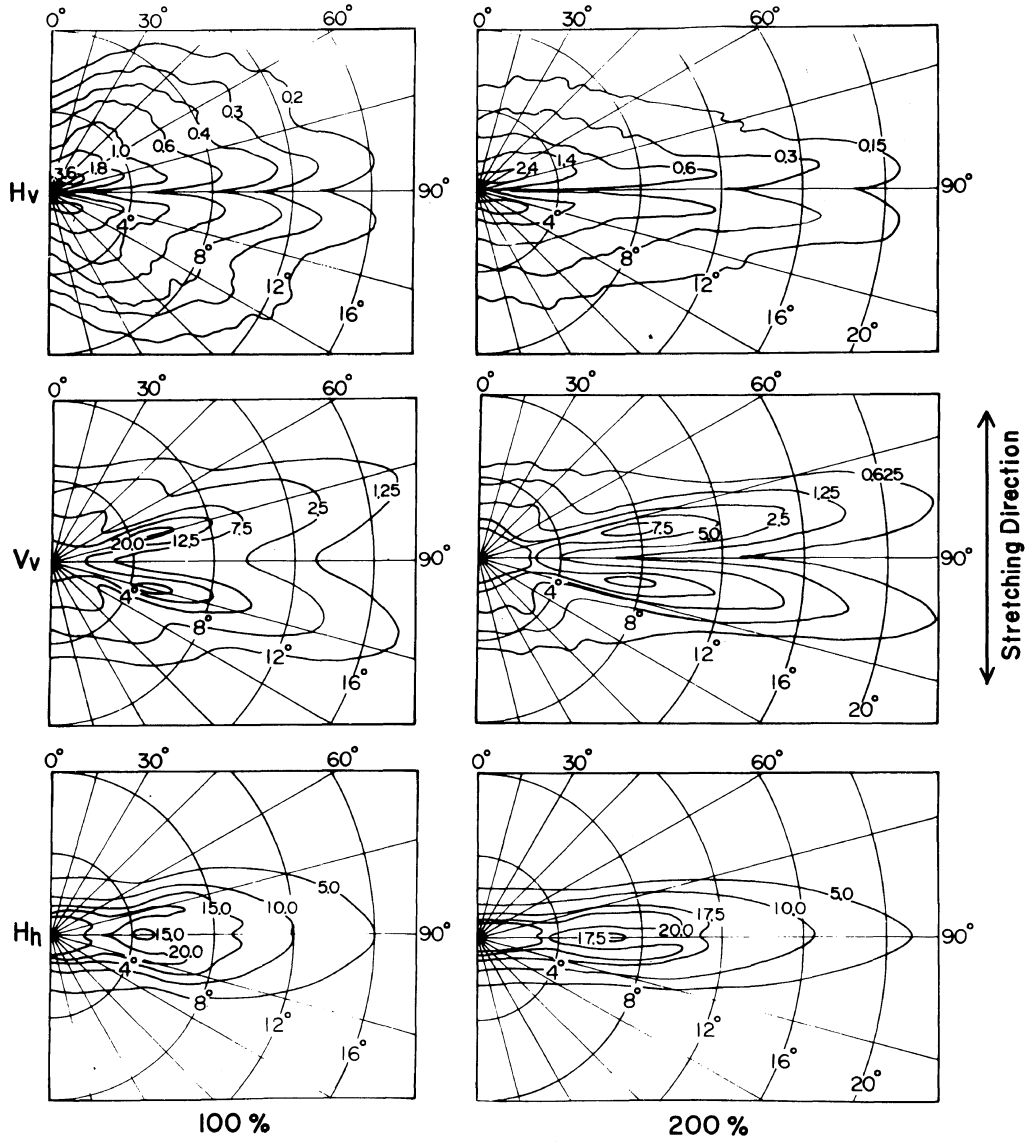

Figure 13. Contour maps of scattered intensity distribution of a specimen B in deformed states of elongation ratios, 100 and 200%, under H_v, V_v, and H_h polarization conditions.

the *b*-axis. This is because the H_v scattered intensity calculated from the above model becomes zero at $\theta=0°$ and $\mu=n\pi/2$ ($n=0\sim3$). These H_v scattering patterns in Figure 12 are rather close to the patterns calculated by Stein and Hashimoto in terms of an affine deformation of the spherulites having the disorder of optical axes orientation in the angular distribution.[22] In their calculation, the magnitude of the orientation fluctuation was also considered to be dependent on the position within the deformed spherulite using a simple assumption of an ellipsoidal variation. However, the deformation mechanism of nylon 6 spherulites contains still essentially unresolved problems and thus a more detailed discussion on the study of oriented crystallization under uniaxial stretching is necessary on the basis of the precise data of the distribution of the light scattered intensity.

CONCLUSIONS

The orientation distribution functions of the reciprocal lattice vectors of the (200) and (002) crystal planes for two specimens having different crystallinities, 47% and 28%, can be obtained by the X-ray diffraction technique. As for the specimen at crystallinity 47%, the functions of the (200) and (002) crystal planes have a maximum at $\theta_j=0°$ and 90°, respectively. On the other hand, as for the specimen at crystallinity 28%, both these functions have maxima at $\theta_j=90°$. This strange phenomenon is analyzed using a deformation model of nylon 6 spherulites associated with the orientation of crystal lamellae including untwisting and with the delayed reorientation of crystallites within the oriented lamella. As a result, this is due to the difference of the orientation mode of the crystallites, two types of the crystal *b*-axis orientation; (a) the *b*-axis orientation associated with rotation of the crystallites around their own *c**-axis designating the axis perpendicular to the *a*- and *c*-axes and (b) the *b*-axis orientation associated with random rotation of the crystallites around their own *b*-axis. The type (a) orientation is indicated in the case of a high degree of crystallinity such as 47%, while the type (b) orientation predominates in the case of a lower degree of crystallinity such as 28%.

The light scattering patterns from the two specimens are found to resemble each other in the undeformed and deformed states, and this is quite in contrast to the orientation modes of the (200) and (002) crystal planes. In order to observe detailed data concerning the distribution of scattered light intensity, the light scattering apparatus was manufactured on trial; the scanning bench supporting the photomultiplier can be moved horizontally at a desired fixed angle between the bench and the horizontal direction. The angle can be changed from $-5°$ to 35° at proper intervals. By using this apparatus, it is unnecessary to rotate the polarizer, sample, and analyzer to measure the distribution of scattered intensity. The contour maps of the scattered intensity distribution provide detailed information on the morphology and deformation mechanism of nylon 6 spherulites. Consequently, the nylon 6 spherulites are considered to be rather close to the spherulites having the disorder of the optical axis orientation in the angular distribution. The effect of the angular disorder becomes evident by measuring the scattered intensity distribution from deformed states.

Acknowledgment. The authors are indebted to Prof. Kawai, Faculty of Engineering, Kyoto University for his valuable suggestions. Thanks are also due to Associate Professor Nomura, Faculty of Textile Science, Kyoto University of Industrial Arts and Textile Fibers, for his valuable comments.

REFERENCES

1. S. Nomura, A. Asanuma, S. Suehiro, and H. Kawai, *J. Polym. Sci., A-2*, **9**, 1991 (1971).
2. S. Nomura, M. Matsuo, and H. Kawai, *J. Polym. Sci., Polym. Phys. Ed.*, **10**, 2489 (1972).
3. M. Matsuo, H. Hattori, S. Nomura, and H. Kawai, *J. Polym. Sci., Polym. Phys. Ed.*, **14**, 223 (1976).
4. R. J. Roe and W. R. Krigbaum, *J. Chem. Phys.*, **40**, 2608 (1964).
5. W. R. Krigbaum and R. J. Roe, *J. Chem. Phys.*, **41**, 737 (1964).
6. R. J. Roe, *J. Appl. Phys.*, **36**, 2024 (1965).
7. M. Matsuo, K. Hirota, K. Fujita, and H. Kawai, *Macromolecules*, **11**, 1000 (1978).
8. M. Matsuo, F. Ozaki, H. Kurita, S. Sugawara, and T. Ogita, *Macromolecules*, **13**, 1187 (1980).
9. A. Keller, *J. Polym. Sci.*, **17**, 291 (1955).
10. F. Khoury, *J. Polym. Sci.*, **33**, 389 (1958).
11. C. R. Lindergren, *J. Polym. Sci.*, **40**, 181 (1961).
12. K. Masuzawa, *Kobunshi Kagaku*, **15**, 14 (1958).
13. A. Keller, *J. Polym. Sci.*, **17**, 351 (1955).
14. For example, W. H. Chu, and D. E. Horne, *J. Polym. Sci., Polym. Phys. Ed.*, **15**, 303 (1977).
15. K. Sasaguri, S. Hoshino, and R. S. Stein, *J. Appl. Phys.*, **35**, 47 (1964).
16. P. Erhardt, K. Sasaguri, and R. S. Stein, *J. Polym. Sci., C*, **5**, 179 (1964).
17. P. Erhardt and R. S. Stein, *J. Polym. Sci., B*, **3**, 553 (1965).
18. T. Oda and R. S. Stein, *J. Polym. Sci., A-2*, **10**, 685 (1972).
19. A. J. Nelder and Mead, *Comput. J.*, **7**, 308 (1965).
20. R. S. Stein and W. H. Chu., *J. Polym. Sci., A-2*, **8**, 1137 (1970).
21. T. Hashimoto and R. S. Stein, *J. Polym. Sci., A-2*, **9**, 1747 (1971).
22. R. S. Stein and T. Hashimoto, *J. Polym. Sci., A-2*, **9**, 517 (1971).